SORT 45 (2) July-December 2021, 143-162 DOI: 10.2436/20.8080.02.113

Bayesian hierarchical nonlinear modelling of intra-abdominal volume during pneumoperitoneum for laparoscopic surgery

Gabriel Calvo[1], Carmen Armero[1], Virgilio Gómez-Rubio[2] and Guido Mazzinari[3]

Abstract

Laparoscopy is an operation carried out in the abdomen through small incisions with visual control by a camera. This technique needs the abdomen to be insufflated with carbon dioxide to obtain a working space for surgical instruments' manipulation. Identifying the critical point at which insufflation should be limited is crucial to maximizing surgical working space and minimizing injurious effects. A Bayesian nonlinear growth mixed-effects model for the relationship between the insufflation pressure and the intra–abdominal volume generated is discussed as well as its plausibility to represent the data.

MSC: 62P10, 62F25.

Keywords: Intra-abdominal pressure, logistic growth function, Markov chain, Monte Carlo methods, random effects.

1. Introduction

Laparoscopy is an operation carried out in the abdomen or pelvis through small incisions with the help of a camera. It is performed by insufflating CO_2 into the abdomen

[1] Department of Statistics and Operations Research, Universitat de València, Carrer Doctor Moliner 50, 46100, Burjassot, Spain.

[2] Departamento de Matemáticas, Escuela Técnica Superior de Ingenieros Industriales, Universidad de Castilla-La Mancha, Avda, de España s/n, 02071, Albacete, Spain.

[3] Research Group in Perioperative Medicine and Department of Anaesthesiology, Hospital Universitari i Politècnic la Fe, Avinguda de Fernando Abril Martorell 106, 46026, València, Spain.

Received: June 2021.
Accepted: November 2021.

that yields a working space, i.e., pneumoperitoneum, and passing surgical instruments through small incisions using a camera to have external visual control of the procedure (Neugebauer et. al., 2010). Laparoscopy has been gaining ground since its inception because it is associated with less morbidity than the traditional method performed through a single, larger skin incision (Pache et al., 2017).

The introduction of CO_2 into the abdomen is operated by medical devices, i.e., laparoscopic insufflators, through small plastic tubes, i.e. trocars, inserted in the patient's abdominal wall. Laparoscopy technological development has been limited to improvements in camera image quality, whereas little innovation has been made in insufflation devices (Colon Cancer Laparoscopic or Open Resection Study Group, 2009).

The CO_2 insufflation pressure, i.e., intra–abdominal pressure (*IAP*), is set manually on the insufflator by the surgical team. *IAP* is measured in millimeters of mercury (mmHg), and the usual figures during laparoscopic surgery range between 12 and 15 mmHg. Although international guidelines recommend working with the lowest *IAP* value that ensures an adequate working space, the standard practice is still to initially set the *IAP* value without further adjustments regardless of the amount of generated intra–abdominal volume (*IAV*) (Neudecker et al., 2002), measured in litres (L). Operating at such high *IAP* increases perioperative morbidity since it leads to decrease abdominal blood perfusion, greater postoperative pain, peritoneal injury, and increased risk of pulmonary complications.

The abdominal compartment shows an anisotropic behaviour during pneumoperitoneum which is explained by its combination of rigid borders, e.g., spine, rib cage, and pelvis, and semirigid borders, e.g., abdominal wall muscles and the diaphragm (Becker et al., 2017). Initially, marginal gains in volume in response to pressure increments are proportional. In other words, the abdominal compliance (C_{abd}), which defines the change in volume determined by a change in pressure, follows an approximately linear relationship (Mulier et al., 2009). According to biomechanics laws, the yield stress point is eventually reached, after which applying additional pressure leads to diminishing gains in volume (Forstemann et al., 2011). Identifying this critical point at which insufflation should be limited is crucial to maximizing surgical working space while minimizing injurious *IAP* effects.

The abdomen pressure–volume dynamics during pneumoperitoneum has been discussed in previous papers (Diaz-Cambronero et al., 2019, 2020; Mazzinari et al., 2020, 2021). These studies suggest the adequacy of an increasing sigmoidal model for describing the relationship between both variables. Our aim in this work is twofold. On the one hand, we want to estimate such a model to gain knowledge about the relationship between *IAP* and *IAV*, especially about the parameters that determine the different growth stages of the process in accordance with the specific characteristics of the individuals in the target population. On the other hand, the second goal of the paper is to discuss the quality of the fit of the model to the data. This is a relevant question since the logistic growth curve is a previously used model for the topic. The hypothesis is that, in a personalised medicine environment, patient responses to insufflation can be estimated and

predicted so that an ideal *IAP* value could be determined to optimise *IAV* with the lowest risks of potential negative effects.

The statistical framework of this study is that of nonlinear growth mixed-effects models, also known as hierarchical nonlinear growth models. They have a long and important scientific tradition for describing biological, medical, and environmental growth phenomena such as pharmacokinetics (Giltinan, 2006), epidemiology (Lindsey, 2001), physiological-response processes (Peek et al., 2002), or forestry (Fang and Bailey, 2001) among others. One of the major appeals of these models is that their parameters contain direct and intuitive information on the process under study. This fact generates a multifaceted knowledge about the phenomena in question of great scientific value (Davidian, 2008).

Data for the study come from a repeated measures design (Lindstrom and Bates, 1990). In our case, the variable of interest *IAV* is measured for each individual with regard to different *IAP* values. This design generates two types of data: data from the same individual and data from several individuals. Random effects in these models are essential elements to glue together the different observations of the same individual as they could be considered as a within-individual variation (Laird and Ware, 1982).

The statistical analysis of the problem has been carried out using Bayesian inference. This statistical methodology accounts for uncertainty in terms of probability distributions (Loredo, 1989, 1992) and uses Bayes' theorem to update all relevant information. The Bayesian approach simplifies the implementation and interpretation of mixed effects models. The conditional formulation of this type of model, which explicitly includes random effects in the conditional mean, allows individual and population inferences to be made. This is due to the simplicity process of integrating out the random effects of the model, that is, moving from the conditional formulation of the model to its marginal formulation (Lee and Nelder, 2004). This feature of Bayesian models is of utmost importance in the case of growth models because it expresses in a natural probabilistic way all information about the parameters and other relevant features of the growth process through the respective posterior distribution. Furthermore, model checking can be conducted in a straightforward way to detect possible systematic bias in the model. This is particularly important for medical applications to avoid patients from receiving a suboptimal medical treatment.

The paper is organised as follows. Section 2 presents the data with a brief description that emphasises the particular features of the repeated-means design through the number of observations per individual and their *IAV* trajectories according to the *IAP* values. Section 3 introduces and formulates the statistical modelling. Section 4 accounts for posterior inferences and prediction. Section 4.1 discusses the posterior distribution of the estimation process. Sections 4.2 and 4.3 contain, respectively, some relevant results of clinical interest at specific individual levels and in general terms for different population groups. Section 5 deals with model checking by means of the cross-validated predictive density. The paper ends with an overview of the results and some conclusions.

2. Intra-abdominal volume and intra-abdominal pressure data

The data for the current modelling come from a previously published individual patient meta–analysis (Mazzinari et al., 2021) that included experimental information from three previous homogeneous clinical studies (Mazzinari et al., 2020; Diaz-Cambronero et al., 2019, 2020). All patients in these studies underwent a standardized pneumoperitoneum insufflation at a constant low flow, i.e., 3 $\mathrm{L\,min^{-1}}$, under deep neuromuscular block with a posttetanic count (PTC) between one and five assessed by quantitative monitoring. The insufflation was carried out through a leakproof trocar up to an IAP of 15mmHg for abdominal wall prestretching and then stepwise changes in IAP in the 8 to 15 mmHg pressure range were recorded. In all studies, patients' legs were placed in padded leg-holder supports with hips flexed before the initial insufflation.

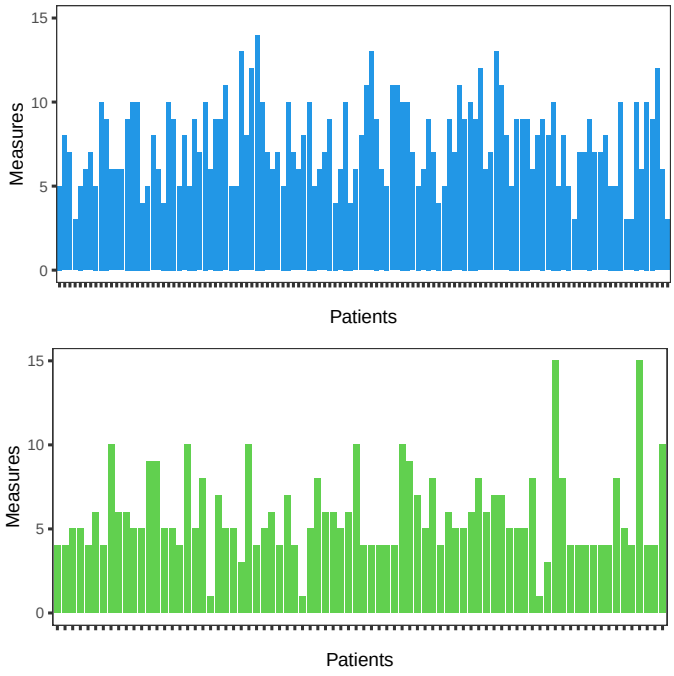

Figure 1. *Number of repeated measures in the men's group (top panel) and in the women's group (bottom panel). Each bar corresponds to a person and its ordinate is the number of measurements of that person during the study. Patients are ordered according to their age from youngest to oldest.*

The original databank had information on 204 patients, but 6 patients presented missing information on IAP, IAV, and/or age values. There are very few individuals whose missing observations do not appear to have been generated by non-ignorable mechanisms. For this reason, we decided to eliminate them directly and not engage in a very unhelpful imputation process. The final databank has 198 patients, 118 men and 80

women, and a total of 1 361 observations. We have a repeated measures design with a very different number of observations per individual: from individuals with only one observation to individuals with 15. Figure 1 shows the number of repeated measures for the group of men and women in order of age. It is interesting to note that women have in general less measurements than men in all ages.

The data have a very wide age range. The youngest patient is 23 years old and the oldest is 92, with a mean age of 64.65 years. In the men's group, the minimum and maximum also are 23 and 92, respectively, and their average is 64.49 years. Women have a minimum age of 34 and a maximum of 85, and their mean is 64.87 years.

IAP values range between 0 and 16 mmHg, and *IAV* values between 0.5 and 13 L. Figure 2 shows a spaghetti plot of *IAV* for men and women. They all show a fairly similar pattern of the *IAV* with *IAP*, although a greater range of values is observed in men, especially in large values of *IAP*. In both groups there are individuals with different behaviour but men behave more homogeneously than women.

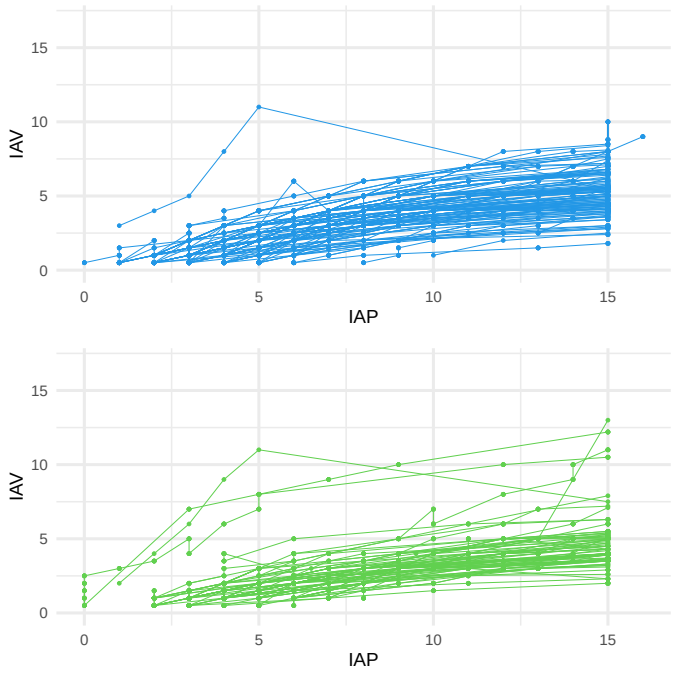

Figure 2. *IAV profiles (in L) according to IAP (in mmHg) for men (top panel) and women (bottom panel) in the sample.*

3. Logistic growth mixed-effects modelling

Let the nonlinear mixed-effects model for the response random variable IAV_{ij} that records the intra-abdominal volume value for individual i, $i = 1,\ldots,n$ with standardized intra-abdominal pressure value IAP_{ij}, $j = 1,\ldots,J_i$, defined in terms of a conditional normal

distribution as follows

$$(IAV_{ij} \mid \mu_{ij}, \sigma^2) \sim \mathrm{N}(\mu_{ij}, \sigma^2), \tag{1}$$

where μ_{ij} is the mean of the *IAV* value of a patient with IAP_{ij} value and can be expressed in terms of the conditional logistic growth function

$$(\mu_{ij} \mid a_i, b_i, c_i, IAP_{ij}) = \frac{a_i}{1+\exp\{-(b_i + c_i IAP_{ij})\}}, \tag{2}$$

with parameters a_i, b_i, and c_i determining the growth of the function, and σ^2 the unknown variance associated to the random measurement error of the normal (1).

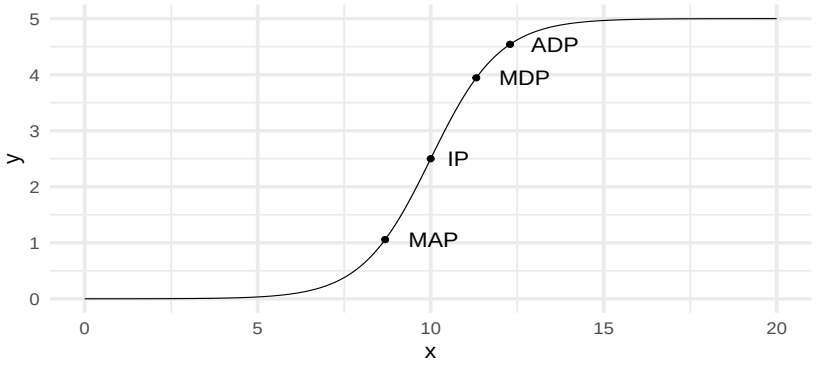

Figure 3. *Graphics of the logistic growth function* $5/[1+exp\{-(-10+x)\}]$*, the subsequent asymptotic value, and its MAP, IP, ADP, and MDP points.*

The logistic growth model for μ_{ij} has important features which are very valuable to better understand the relationship between *IAP* and *IAV* (Davidian, 2008):

- It is an increasing sigmoid function (see Figure 3), or *S*-curve, whose name comes from its shape and was introduced by the mathematician Pierre-François Verhulst in the 19th century to study the growth of populations in autocatalytic chemical reactions (Cramer, 2004).
- The asymptotic value of *IAV* when *IAP* goes to infinity is a_i.
- The inflection point (*IP*), where the curve changes from being concave downward to concave upward and therefore it is the point at which the acceleration of the process switches from positive to negative, is $-b_i/c_i$ for *IAP*. The value of *IAV* at this point is $a_i/2$.
- The maximum acceleration and deceleration point, *MAP* and *MDP* respectively, have the following *IAP* and *IAV* coordinates, $((-(\ln(2+\sqrt{3})+b_i)/c_i, a_i/(3-\sqrt{3}))$ and $(-(-\ln(2-\sqrt{3})+b_i)/c_i, a_i/(3+\sqrt{3}))$.

- The asymptotic deceleration point (*ADP*) is calculated by equalling the fourth derivative to 0. It is located after the maximum deceleration point, and it indicates the point in which the acceleration is negative but close to 0. Therefore, it is expected that the increase of the function is not of much practical interest. The *ADP* is $-(\ln(5-2\sqrt{6})+b_i)/c_i$ for *IAP*. The value of *IAV* at this point is $a_i(3+\sqrt{6})/6$.

By way of illustration, Figure 3 shows the graph of the logistic growth model $y = 5/[1+\exp\{-(-10+x)\}]$ with generic variables x and y, and the location on the graph of the special points described above.

Hierarchical modelling for parameters a_i and b_i was based on expert information and connected them with standardized age and gender covariates. Parameter c_i was associated to covariate gender. We discarded its connection to covariate age as a consequence of a previous analysis of variable selection that we will discuss later. Furthermore, a_i and b_i also included a random effect specifically associated to each individual that allow to connect all their repeated observations. We have not included any random effect in the modelling of the parameter c_i because it would generate a random interaction term with the *IAP* values that would be difficult to understand and justify. Following this reasoning, our model would be

$$a_i = \beta_0^{(a)} + u_i^{(a)} + \beta_W^{(a)} I_W(i) + \beta_A^{(a)} Age_i, \tag{3}$$

$$b_i = \beta_0^{(b)} + u_i^{(b)} + \beta_W^{(b)} I_W(i) + \beta_A^{(b)} Age_i, \tag{4}$$

$$c_i = \beta_0^{(c)} + \beta_W^{(c)} I_W(i), \tag{5}$$

where $\boldsymbol{\beta}_0 = (\beta_0^{(a)}, \beta_0^{(b)}, \beta_0^{(c)})^\intercal$ stands for the common intercept with the men group being the reference group, $I_W(i)$ is the indicator variable with value 1 if individual i is a woman and 0 otherwise, $\boldsymbol{\beta}_W = (\beta_W^{(a)}, \beta_W^{(b)}, \beta_W^{(c)})^\intercal$ and $\boldsymbol{\beta}_A = (\beta_A^{(a)}, \beta_A^{(b)})^\intercal$ are the vector of regression coefficients associated with individual i being a woman and their standardized age, respectively. Random effects $u_i^{(a)}$ and $u_i^{(b)}$, $i = 1, \ldots, n$, are assumed conditional independent given σ_a^2 and σ_b^2 and normally distributed according to $(u_i^{(a)}|\sigma_a^2) \sim \mathrm{N}(0, \sigma_a^2)$ and $(u_i^{(b)}|\sigma_b^2) \sim \mathrm{N}(0, \sigma_b^2)$.

The Bayesian model is completed with the elicitation of a prior distribution for the parameters and hyperparameters $\boldsymbol{\theta} = (\boldsymbol{\beta}_0, \boldsymbol{\beta}_W, \boldsymbol{\beta}_A, \sigma, \sigma_a, \sigma_b)^\intercal$ of the model. We assume prior independence between them and select the uniform distribution $\mathrm{U}(0,10)$ for all standard deviation terms. The elicited marginal prior distributions for $\beta_0^{(a)}$ and $\beta_0^{(c)}$ are $\mathrm{U}(0,20)$ and $\mathrm{U}(0,10)$, respectively. These uniform distributions are sufficiently large to cover generously the whole range of possible values of both parameters. A normal distribution $\mathrm{N}(0, 10^2)$ is selected for $\beta_0^{(b)}$, $\beta_W^{(a)}$, $\beta_W^{(b)}$, $\beta_W^{(c)}$, $\beta_A^{(a)}$, and $\beta_A^{(b)}$ to allow the parameters to move freely between a wide range of positive and negative values.

4. Posterior inferences and predictions

4.1. Posterior distribution

The relevant quantities in the inferential process are the parametric vector $\boldsymbol{\theta}$ and the set of random effects associated to the individuals in the sample $\boldsymbol{u} = (\boldsymbol{u}_1, \ldots, \boldsymbol{u}_n)^\top$, where $\boldsymbol{u}_i = (u_i^{(a)}, u_i^{(b)})$. The posterior distribution $\pi(\boldsymbol{\theta}, \boldsymbol{u} \mid \mathcal{D})$, where $\mathcal{D}$ represents the observed *IAV* and *IAP* data of all individuals in the sample as well as their age and gender, contains all the relevant information of the problem and it is usually the starting point of all relevant inferences. It was approximated by means of Markov Chain Monte Carlo (MCMC) simulation methods through the JAGS software (Plummer, 2003). For the estimated model, we ran three parallel chains with 1,000,000 iterations and a burn-in of 500,000. Chains were also thinned by storing every 1,000th iteration to reduce autocorrelation in the sample. Convergence to the joint posterior distribution was guaranteed by visualising every autocorrelation function plot by means of `mcmcplot` package for the R software and assuring an effective number of independent simulation draws greater than 100. For the sake of reproducibility we have generated a fictitious databank, which together with the R code for the analyses is available as supplementary material here https://github.com/gcalvobayarri/intra_abdominal_volume_model.git.

Table 1. *Posterior summaries (mean, standard deviation and* 95% *credible interval) for the parameters and hyperparameters of the logistic growth model with covariates gender and standardized age.*

	Logistic growth model		
Parameters	mean	sd	$CI_{0.95}$
$\beta_0^{(a)}$	5.729	0.377	(4.968, 6.452)
$\beta_W^{(a)}$	−0.418	0.259	(−0.927, 0.095)
$\beta_A^{(a)}$	0.101	0.124	(−0.145, 0.349)
σ_a	1.670	0.090	(1.501, 1.860)
$\beta_0^{(b)}$	1.080	0.181	(0.730, 1.440)
$\beta_W^{(b)}$	−0.270	0.125	(−0.517, −0.028)
$\beta_A^{(b)}$	0.134	0.054	(0.026, 0.241)
σ_b	0.650	0.041	(0.572, 0.736)
$\beta_0^{(c)}$	2.260	0.120	(2.029, 2.503)
$\beta_W^{(c)}$	−0.264	0.082	(−0.431, −0.101)
σ	0.490	0.011	(0.469, 0.513)

Table 1 summarizes $\pi(\boldsymbol{\theta}, \boldsymbol{u} \mid \mathcal{D})$. The posterior mean of $\beta_0^{(a)}$ and $\beta_0^{(b)}$ provides an approximate overall assessment of the baseline values of a_i and b_i for male patients. In

the case of the asymptotic value a_i, it decreases by about 0.418 in the female group (although this estimation has a lot of uncertainty), and shows a slight positive trend with age. Differences between individuals are relevant as it can be seen from the estimation of the standard deviation of the random effect in a_i, 1.67. The parameter b_i has an approximate basal value of 1.08 in the men group, which decreases by -0.27 units in the women group. Age also has a positive estimation and the random effect associated to individuals are also important for b_i, especially because this term appears on an exponential scale and negative sign in the quotient of the growth curve. Finally, the posterior mean for the c_i term is about 2.26 in the men group and decreases in 0.264 units in the group of women. The posterior mean of the standard deviation associated to the measurement error is not very large but it does have a very high accuracy. The fact that the *IAP* value of the *IP*, *ADP*, *MAP* and *MDP* of individual i depends on b_i and c_i proportionally to $-b_i/c_i$, and that the estimated coefficient associated to age is positive for b_i implies that the relationship of the *IP*, *ADP*, *MAP* and *MDP* for *IAP* coordinate with age is negative but barely important.

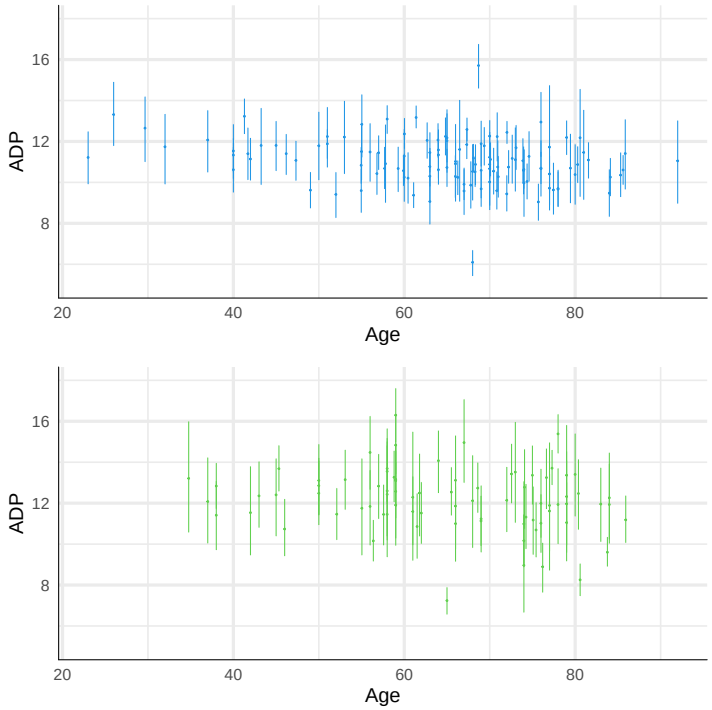

Figure 4. *Posterior mean and 95% credible interval of the ADP (IAP value) of the men (top panel) and the women (bottom panel) in the sample. Patients are ordered in the x-axis in terms of their age.*

As mentioned above, the posterior distribution is the starting point for the analysis of the different outcomes of interest in the study. In the following, we will present different

results that may be useful to better understand the relationship between *IAV* and *IAP* at both the individual and population level and thus be able to answer the scientific questions raised by the study. But first we would like to make a brief comment on the variable selection process discussed above for parameter c_i of the growth model. In this context, we considered different modelling approaches for c_i with regard to covariate gender. The Deviance Information Criterion (Spiegelhalter et al., 2002) was used for model comparison and according to this criterion the best model was the one with only the gender covariate and a common population term in parameter c_i as stated before.

4.2. Posterior individual outcomes

The basic inferential process allows the Bayesian methodology to obtain information both individually and in terms of the target population. In the following we focus on *ADP*. The mean of the *IAP* value of *ADP* for individual i, ADP_i, depends on b_i and c_i, which in turn depends on $(\boldsymbol{\theta}, \boldsymbol{u}_i)$. Consequently, we can compute the posterior distribution of the true ADP_i of each individual i in the sample from the subsequent posterior distribution $\pi(\boldsymbol{\theta}, \boldsymbol{u}_i \mid \mathcal{D})$. Figure 4 shows the posterior *ADP* mean and a 95% credible interval for the individuals in the sample ranked by age. The first thing that is striking in both graphs is the great difference in both the men and women groups in the range of credibility intervals, which is mainly explained by the differences in the number of repeated observations for each of them.

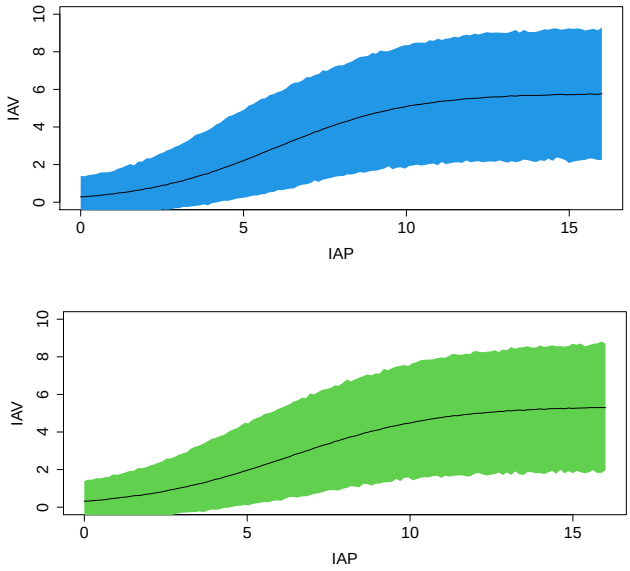

Figure 5. *Posterior predictive mean of the IAV and 95% predictive interval with regard to IAP values for a man (top panel) and a woman (bottom panel) aged 64.65 years (the sample mean).*

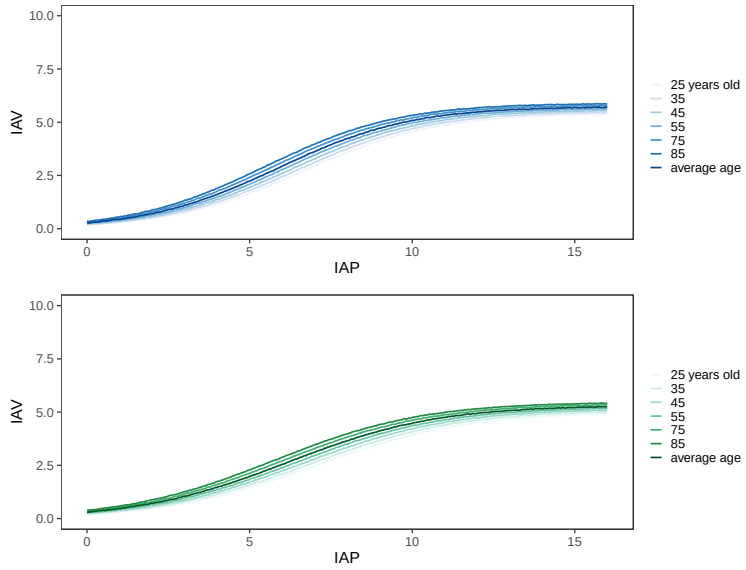

Figure 6. *Posterior predictive mean of the IAV with regard to IAP values for a man (top panel) and a woman (bottom panel) stratified by age.*

Prediction of observations for new individuals of the target population is an important issue that Bayesian statistics approaches in a natural way. The posterior predictive distribution of the random variable $Y_{n+1,j}$ that records the *IAV* value for a new individual, $n+1$, of the population with regard to their *IAP*, standardized age and gender values, which from now on we will denote by $\boldsymbol{x}_{n+1,j}$, depends on the conditional model in (1) and the posterior distribution $\pi(\boldsymbol{\theta}, \boldsymbol{u}_{n+1} \mid \mathcal{D})$, where $\boldsymbol{u}_{n+1}$ are the random effects associated to that individual $n+1$. It is computed as follows

$$f(y_{n+1,j} \mid \boldsymbol{x}_{n+1,j}, \mathcal{D}) = \int f(y_{n+1,j} \mid \boldsymbol{x}_{n+1,j}, \boldsymbol{\theta}, \boldsymbol{u}_{n+1})\, \pi(\boldsymbol{\theta}, \boldsymbol{u}_{n+1} \mid \mathcal{D})\, \mathrm{d}(\boldsymbol{\theta}, \boldsymbol{u}_{n+1}), \qquad (6)$$

where the posterior $\pi(\boldsymbol{\theta}, u_{n+1} \mid \mathcal{D})$ factorizes in terms of the marginal posterior distribution $\pi(\boldsymbol{\theta} \mid \mathcal{D})$ and the conditional distributions for the random effects $(u^a_{n+1} \mid \sigma^2_a) \sim N(0, \sigma^2_a)$ and $(u^b_{n+1} \mid \sigma^2_b) \sim N(0, \sigma^2_b)$. Figure 5 shows the posterior predictive mean and a 95% predictive interval for the *IAV* value of a new individual of the target population with age 64.65, the sample mean of the data, with respect to their *IAP* value and their gender. Both groups behave very similarly. The stabilisation of the values of *IAV* in both groups can be clearly seen, as well as the variability associated with the predictive processes, which is always greater in comparison with the estimation processes themselves. Finally, Figure 6 shows the posterior predictive mean for the response *IAV* variable with regard to *IAP* values of men and women with different ages. Of course, as we observed with the approximate posterior distribution of $\beta^{(b)}_A$ in the Table 1, a positive relationship

between *IAV* and age can be observed in the graphic, but it is very mild and possibly not very relevant for practical purposes in clinical scenarios.

4.3. Posterior population outcomes

Random effects connect the different repeated measures of the same individual in the statistical model and allow for the computation of individual-specific outcomes. We would also like to be able to have not only that individual information, but also outcomes that can provide general information about the target population. This aim implies to work with the marginal formulation of the model in (1) and (2) which we would obtain by integrating out the random effects of the conditional modelling as follows

$$f(y_{ij} \mid \boldsymbol{x}_{ij}, \boldsymbol{\theta}) = \int f(y_{ij} \mid \boldsymbol{x}_{ij}, \boldsymbol{\theta}, \boldsymbol{u})\, f(\boldsymbol{u} \mid \boldsymbol{\theta})\, \mathrm{d}\boldsymbol{u} = \int \mathrm{N}(\mu_{ij}, \sigma^2)\, f(\boldsymbol{u} \mid \boldsymbol{\theta})\, \mathrm{d}\boldsymbol{u}. \qquad (7)$$

This marginal formulation only depends on the parameter and hyperparameters of the model $\boldsymbol{\theta}$ and is the basis for the computation of any feature of this marginal model. For simplicity, we only focus on the true asymptotic *IAV* value and the true asymptotic deceleration point *ADP* for a patient with an average age.

Figure 7 shows the posterior distribution of the asymptotic *IAV* for men and women aged 64.65 years (the mean of the sample). There is not much difference between the two distributions. An estimation of the asymptotic *IAV* in the group of men is 5.60 L. while in the group of women it is 5.25 L. Figure 8 shows the joint posterior distribution, in terms of contour lines, of the *ADP* pressure point and the subsequent volume value for men and women aged 64.65 years (the sample mean) as well as the marginal distributions of both quantities. Posterior mean for the *ADP*'s pressure and volume is 10.06 mmHg. and 5.05 L. in men aged 64.65, and 10.87 mmHg. and 4.74 L. in the group of women with the same age, respectively. A similar analysis is possible for *MAP*, *IP* and *MDP*. However, their posterior results for both coordinates (*IAP* and *IAV*) are proportional to those of *ADP* and their information would be repetitive.

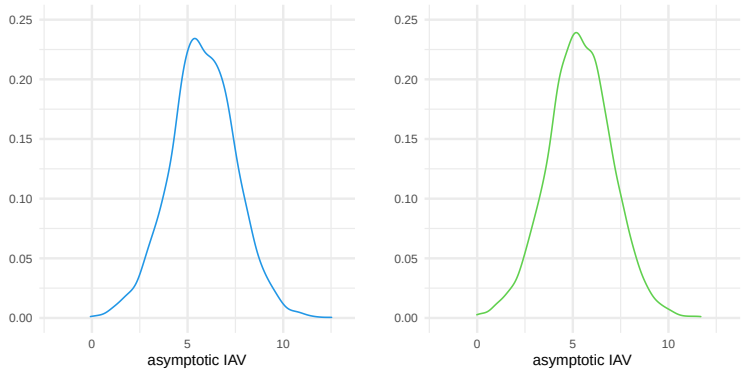

Figure 7. *Posterior distribution of the asymptotic IAV for men (on the left) and women (on the right).*

5. Model checking

Model checking is an essential component of any statistical analysis which has generated an extensive literature within the Bayesian reasoning (Vehtari and Ojanen, 2012). Our interest in this subject focuses on assessing, following the philosophy in Gelman et al (2014), whether the possible shortcomings of our model have a relevant effect on the derived results. We approach model checking via posterior predictive distributions following the ideas by Box (1980), who states that prediction (and not estimation) enables "criticism of the entertained model in light of current data".

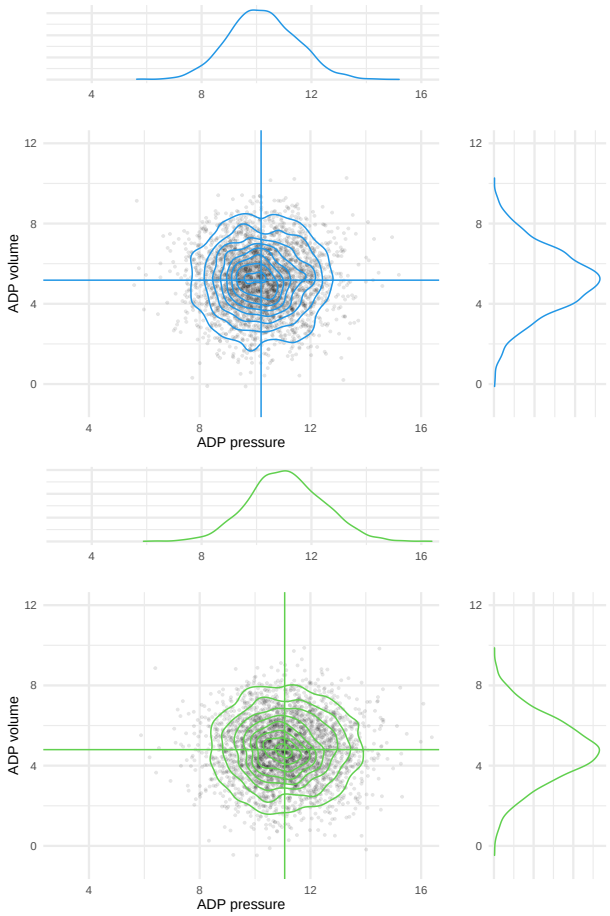

Figure 8. *Joint posterior distribution and contour lines of the IAP and IAV coordinates for the true ADP and posterior marginal distribution for each of both quantities for men (top panel) and women (bottom panel) aged 64.65 years (the sample mean). The horizontal and vertical lines represent the approximate posterior mean of IAV − ADP and the approximate posterior mean of IAP − ADP, respectively.*

We check our model through the cross-validated predictive density Gelfand, Dey and Chang (1992) defined as the conditional posterior density of a future *IAV* value $y_{ij}^{(rep)}$ for individual i, $i = 1,\ldots,n$ with standardized *IAP* value x_{ij} of a replicate experiment

$$f(y_{ij}^{(rep)} \mid \mathcal{D}^{-(ij)}) = \int f(y_{ij}^{(rep)} \mid \boldsymbol{x}_{ij}, \boldsymbol{\theta}, \boldsymbol{u})\, \pi(\boldsymbol{\theta}, \boldsymbol{u} \mid \mathcal{D}^{-(ij)})\, d(\boldsymbol{\theta}, \boldsymbol{u}),$$

where $\mathcal{D}^{-(ij)}$ are all the data in $\mathcal{D}$ except for the observation y_{ij} (leave-one-out (LOO) procedure).

The fundamental idea underlying this proposal assumes that if the estimated model is correct, each observation can be considered as a random value from the cross-validated predictive density Chen, Shao, and Ibrahim (2000). In this framework, we consider two complementary characteristics of such predictive distribution assessed at each observed value y_{ij}. These quantities are the conditional predictive ordinate (CPO) and the cross-validated probability integral (PIT), and are defined as:

$$\begin{aligned} CPO_{ij} &= f(y_{ij} \mid \mathcal{D}^{-(ij)}), \\ PIT_{ij} &= P(Y_{ij}^{(rep)} \leq y_{ij} \mid \mathcal{D}^{-(ij)}). \end{aligned}$$

CPO_{ij} values correspond to the ordinates in the y_{ij} of the cross-validated predictive density. Large CPO_{ij} values support the selected model because indicate a good tuning between the data and the model. PIT_{ij} is the posterior probability that the replicated $(ij)th$ observation is less or equal the subsequent observed value. When the model is well calibrated these probabilities follow a uniform distribution in the unit interval.

The direct implementation of these quantities is computationally very expensive because we would need to approximate as many posterior distributions as we have elements in $\mathcal{D}$. This is not necessary because the application of self-normalized importance sampling allows CPOs and PITs to be approximated from draws of the posterior distribution $\pi(\boldsymbol{\theta}, \boldsymbol{u} \mid \mathcal{D})$ computed with the complete data $\mathcal{D}$ (Gelfand, 1996; Ntzoufras, 2011). Computation of CPOs and PITs was done by means of the R software from the posterior outputs obtained with JAGS.

Figure 9 shows the histogram of CPOs and PITs respectively. The information provided in both cases suggests that the model used has some shortcomings that can be improved. We have some values of the CPO that are small and the PITs do not seem to be uniformly distributed mainly due to a remarkable abundance of values close to zero.

Figure 10 shows how PIT values are distributed along *IAP*. Theoretically, $PIT's$ should be uniformly distributed between 0 and 1 at each *IAP* point. However, from $IAP \approx 6.5$ (vertical red line) to $IAP \approx 14$ PIT values do in general do not exceed 0.5. This behaviour indicates that our model performs well when we work with small values of *IAP*, overpredicts observations of *IAV* for medium and medium-high values of the covariate *IAP*, and finally, it seems to improve with large IAP values.

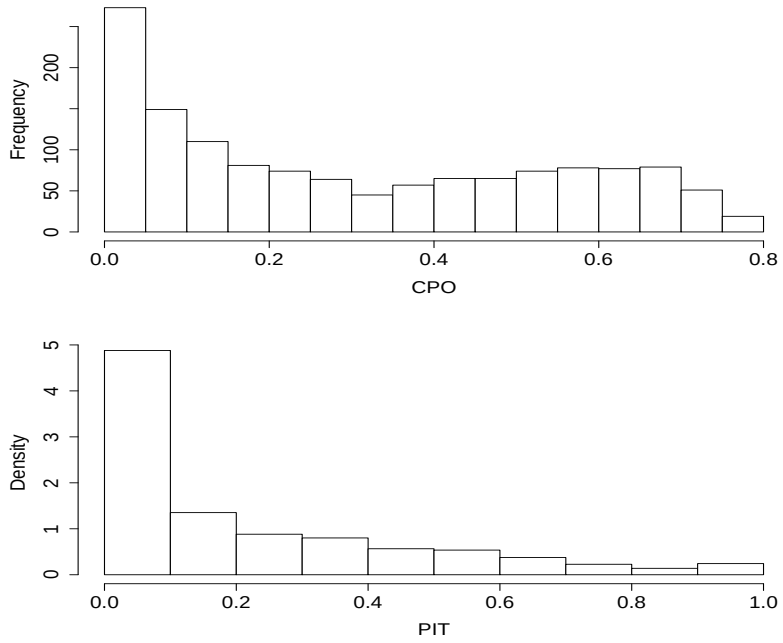

Figure 9. *Histogram of the approximate CPO (on the top) and density histogram of the approximate PIT (in the bottom) quantities for all the observations.*

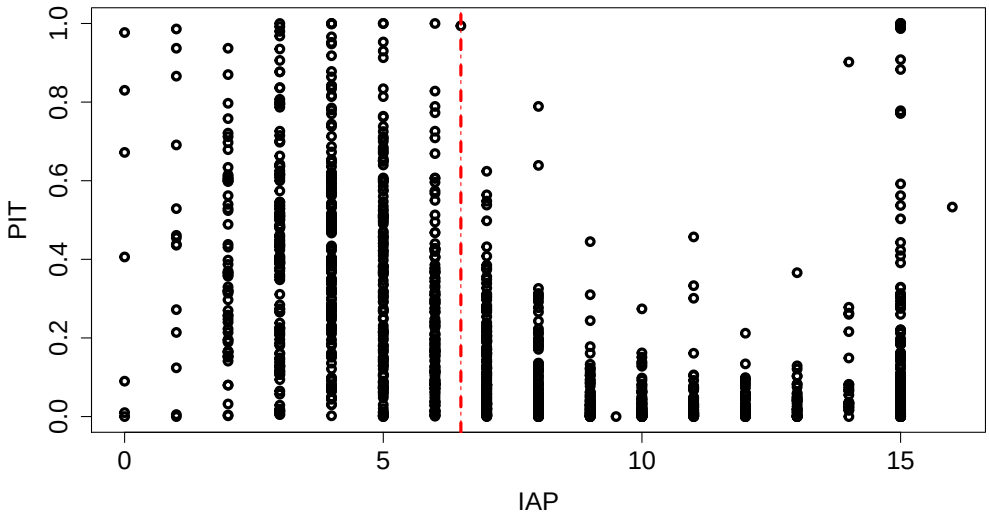

Figure 10. *Distribution of PIT values along the different values of IAP.*

Conclusions

Precision medicine tenets are that different interventions have distinct effects in different people and that this variability can, at least in part, be characterized and predicted (Senn, 2016). In this study we have tried to lay the foundation for the mathematical modeling of the abdomen behaviour during pneumoperitoneum insufflation. We have also parameterized such model to achieve predictive capability based on a few simple baseline characteristics. This is the first step in a precision medicine approach to pneumoperitoneum insufflation for laparoscopic surgery. This process can be potentially scaled up and recursively performed throughout the duration of the surgical intervention to ensure that even if conditions change, we could be able to provide an optimal surgical field to the surgeon while exposing the patient the lowest possible pressure.

With this procedure, we would like to achieve an optimal surgical workspace while minimizing the pressure administered to the patient. In other words, each subject would receive a titrated pressure according to her/his characteristics. Also, the ability to predict where the marginal gain in volume diminishes by deriving critical points on the parameterized curve have an especially interesting clinical potential.

Bayesian inference can provide a suitable inferential framework in this context. First of all, Bayesian hierarchical models are useful to elicit and formulate the different sources of variation and uncertainty of the problem and incorporate suitable terms into the model to account for them. In this particular case, the model includes nonlinear effects through a logistic growth function. As model fitting relies on MCMC methods, inference about particular elements of interest in the model becomes feasible. For example, the logistic growth model has a known parametric form from which some crucial critical points can be derived analytically but inference on these points is far from straightforward. However, the output produced by MCMC during model fitting can be exploited to compute the posterior marginals of these particular points as well as those of the other model parameters. This provides extra information that can be used during the laparoscopic surgery. Inference about these critical points under other inferential frameworks would not be so straightforward.

The most important critical point in our study is ADP, as this controls how much air is insufflated during surgery. From a clinical point of view, when operating on new patients, ADP's predictive distribution can help physicians provide adequate insufflation during laparoscopic surgery.

As we have illustrated, model checking is critical for health applications of statistical methodology as this will allow potential bias to be detected. We believe that the use of the model checking techniques should be widely adopted when relying on statistical models for medical practice to detect and avoid systematic biases in medical treatment (Obermeyer et al., 2019).

The study presented in this paper illustrates a preliminary analysis in which 198 patients have been enrolled. In the future, we aim to conduct a larger trial so that a wider range of patients is represented. Furthermore, other covariates will be recorded and in-

cluded into the model to reduce the uncertainty about the estimates and predictions, and increase the accuracy of insufflation. We plan to refine our model with anthropometric measurements. We are recording not only height and weight, but also waist and hip circumference and abdomen sagittal height to have abdominal, volume and body mass surface and update our model with these new data. Furthermore, data from medical imaging such as abdominal volume estimation based on routine preoperative computerized tomography images or ultrasonic assessment of the abdominal wall thickness and fat component can be explored as covariate alternatives. We will also record the number of previous open and laparoscopic abdominal surgeries, as well as, in the case of women, the number of pregnancies. Finally, models with different assumptions will be considered such as non-homoscedastic models with increasing variability, different types of curves such as the Gompertz curve (Funatogawa and Funatogawa, 2018), or even the inclusion of random effects to assess the possible variability among the different studies.

Acknowledgements

We would like to highlight and thank the work of the editor of the journal and the three anonymous referees who reviewed the paper because their comments and suggestions have greatly improved its quality and clarity. This paper was supported by research grant PID2019-106341GB-I00 funded by Ministerio de Ciencia e Innovación (Spain) and the Project MECESBAYES (SBPLY/17/180501/000491) funded by the Consejería de Educación, Cultura y Deportes, Junta de Comunidades de Castilla-La Mancha (Spain). Gabriel Calvo is also supported by grant FPU18/03101 funded by the Ministerio de Ciencia e Innovación (MCI, Spain). Merck Sharp & Dohme funded the IPPColLapse II study (Protocol Code No. 53607). This is an investigator-initiated study in which the sponsors and funders have no roles in study design, analysis of data, or reporting.

References

Becker, C., Plymale, M. A., Wennergren, J., Totten, C., Stigall, K., Roth, J. S. (2017) Compliance of the abdominal wall during laparoscopic insufflation. *Surgical Endoscopy*, 31, 1947–1951

Box, G. E. P. (1980). Sampling and Bayes's inference in scientific modelling and robustness (with discussion). *Journal of the Royal Statistical Society, Series A*, 143, 383-430.

Chen, M.-H., Shao, Q.-M., and Ibrahim, J. G. (2000). *Monte Carlo Methods in Bayesian Computation*. New York: Springer.

Colon Cancer Laparoscopic or Open Resection Study Group; Buunen, M., Veldkamp, R., Hop, W. C., Kuhry, E., Jeekel, J., Haglind, E., et al. (2009). Survival after laparoscopic surgery versus open surgery for colon cancer: long-term outcome of a randomised clinical trial. *The Lancet Oncology* 10(1), 44–52.

Cramer, J. S. (2004). The early origins of the logit model. *Studies in History and Philosophy of Biological and Biomedical Sciences* 35, 613–626.

Davidian, M. (2008). Non-linear mixed-effects model. In *Longitudinal data analysis*. Chapman and Hall/CRC. p. 121–156.

Diaz-Cambronero, O., Flor Lorente, B., Mazzinari, G., Vila Montañés M, García Gregorio, N,, Robles Hernández, D. et al. (2020). A multifaceted individualized pneumoperitoneum strategy for laparoscopic colorectal surgery: a multicenter observational feasibility study. *Surgical Endoscopy*, 33, 252–260.

Diaz-Cambronero, O., Mazzinari, G., Flor Lorente, B., García Gregorio, N., Robles-Hernández, D., Olmedilla Arnal, L. E. et al. (2020) Effect of an individualized versus standard pneumoperitoneum pressurestrategy onpostoperative recovery: a randomized clinical trial in laparoscopic colorectal surgery. *British Journal of Surgery*, 107, 1605–1614.

Fang, Z. and Bailey, R. L. (2001. Nonlinear Mixed Effects Modeling for Slash Pine Dominant Height Growth Following Intensive Silvicultural Treatments. *Forest Science*, 47, 287–300.

Forstemann, T., Trzewik, J., Holste, J., Batke, B., Konerding, M. A., Wolloscheck, T., Hartung C. (2011). Forces and deformations of the abdominal wall–a mechanical and geometrical approach to the linea alba. *Journal of Biomechanics*, 44, 600–606.

Funatogawa, I., Funatogawa, T. (2018). Nonlinear Mixed Effects Models, Growth Curves, and Autoregressive Linear Mixed Effects Models. In: JSS Research Series in Statistics (ed). *Longitudinal Data Analysis*, pp 99–117. Springer, Singapore.

Gelfand, A. E., Dey, D. K., and Chang, H. (1992). Model determination using predictive distributions with implementation via sampling-based methods. In *Bayesian Statistics* 4 (Eds. J. M. Bernardo, J. O. Berger, A. P. Dawid, and A. F. M. Smith). Oxford: Oxford University Press, 165–180.

Gelfand, A. E. (1996). Model determination using sampling-based methods. In *Markov Chain Monte Carlo in Practice* 4 (Eds. W. Gilks, S. Richardson, and D. Spiegelhalter). Chapman & Hall, 145–161.

Gelman, A., Carlin, J. B., Stern, H. S., Dunson, D. B., Vehtari, A., and Rubin, D. (2014). *Bayesian Data Analysis*, Third Edition. Boca Raton: Chapman and Hall.

Giltinan, D. M. (2006). Pharmacokinetics and pharmacodynamics. In P. Armitageand T. Colton (eds), *Encyclopedia of Biostatistics*, 2nd ed,, pp. 600–606. Wiley, Hoboken, NJ.

Laird, N. M. and Ware, J. H. (1982). Random-Effects for Longitudinal Data. *Biometrics*, 38, 963–974.

Lee, Y. and Nelder, J. A. (2004). Conditional and Marginal Models: Another View . *Statistical Science*, 19(2), 219–238.

Lindsey, J. K. (2001). *Nonlinear Models in Medical Statistics*. Oxford University Press, Oxford.

Lindstrom, M. J. and Bates, D. M. (1990). Nonlinear Mixed Effects Models for Repeated Measures Data. *Biometrics*, 46(3), 673–687.

Loredo, T. J. (1989) From laplace to supernova sn 1987a: Bayesian inference in astrophysics. In: Fougère PF (ed). *Maximum entropy and Bayesian methods*, pp 81–142. Kluwer Academic publishers, Dordrecht.

Loredo, T. J. (1992) Promise of Bayesian inference for astrophysics. In: Feigelson E, Babu G (eds). *Statistical challenges in modern astronomy*, pp 275–297. Springer, New York.

Mazzinari, G., Diaz-Cambronero, O., Alonso-Iñigo, J. M., García Gregorio, N., Ayas-Montero, B. et al. (2020). Intraabdominal pressure targeted positive end-expiratory pressure during laparoscopic surgery: an open-label, nonrandomized, crossover, clinical trial. *Anesthesiology*, 132, 667–677.

Mazzinari, G., Diaz-Cambronero, O., Serpa Neto, A., Martínez Cañada, A., and Rovira, L., Argente Navarro, M. P., et al. (2021). Modeling intra-abdominal volume and respiratory driving pressure during pneumoperitoneum insufflation − a patient-level data meta-analysis. *Journal of Applied Physiology* 130(3), 721–728.

Mulier, J., Dillemans, B., Crombach, M., Missant, C., Sels, A. (2009). On the abdominal pressure volume relationship. *The Internet Journal of Anesthesiology* 21, 1–7. 5221.

Neudecker, J., Sauerland, S., Neugebauer, E. A. M. et al. (2002) The EAES clinical practice guidelines on the pneumoperitoneum for laparoscopic surgery. *Surgical Endoscopy*, 16(7), 1121–43

Neugebauer, E. A. M, Becker, M., Buess, G. F. et al. (2010). EAES recommendations on methodology of innovation management in endoscopic surgery. *Surgical Endoscopy*, 24(7), 1594–1615.

Ntzoufras, I. (2011). *Bayesian modeling using WinBUGS*. John Wiley & Sons.

Obermeyer, Z., Powers, B., Vogeli, C., Mullainathan, S. (2019). Dissecting racial bias in an algorithm used to manage the health of populations. *Science*, 6464 (366), 447–453.

Pache, B., Hübner, M., Jurt, J., Demartines, N., and Grass, F. (2017). Minimally invasive surgery and enhanced recovery after surgery: the ideal combination? *Journal of Surgical Oncology*, 116(5), 613–616.

Peek, M. S., Russek-Cohen, E., Wait, D. A. and Forseth, I. N. (2002). Physiological response curve analysis using nonlinear mixed models. *Oecologia*, 132, 175–180.

Plummer, M. (2003). JAGS: A program for analysis of Bayesian graphical models using Gibbs sampling. In *Proceedings of the 3rd international workshop on distributed statistical computing*. p. 1–10.

Senn, S. (2016). Mastering variation: variance components personalised medicine. *Statistics in Medicine*, 30(7), 966–977.

Spiegelhalter, D. J., Best, N. G., Carlin, B. P. and Van Der Linde, A. (2002). Bayesian measures of model complexity and fit. *Journal of the Royal Statistical Society: Series B (Statistical Methodology)*, 64, 583-639.

Vehtari, A. and Ojanen, J. (2012). A survey of Bayesian predictive methods for model assessment, selection and comparison. *Journal of Biomechanics*, 6, 142–228.